Search for inverse fission of uranium

R. Yanez, W. Loveland, J. Beckerman, and M. Leonard
Department of Chemistry, Oregon State University, Corvallis, Oregon 97331, USA

C. J. Gross, D. Shapira, J. F. Liang, Z. Kohley, and R. L. Varner
Physics Division, Oak Ridge National Laboratory, Oak Ridge, Tennessee 37831, USA

(Received 18 February 2012; published 27 April 2012)

Background: There is a long-term interest in running the fission reaction backward, i.e., studying the "inverse fission" of uranium. The recent availability of beams of n-rich fission fragments has stimulated interest in this endeavor.
Purpose: To search for inverse fission in the reactions ^{124,132}Sn + ^{100}Mo.
Method: In the ^{124}Sn + ^{100}Mo reaction, evaporation residues were searched for using in-beam detection of evaporation residues, in-beam α spectroscopy, and post-irradiation α spectroscopy, while in the ^{132}Sn + ^{100}Mo reaction, the evaporation residue ^{230}U was searched for using post-irradiation α spectroscopy.
Results: No evidence for the occurrence of the inverse fission reactions was found. The upper-limit cross section for the latter reaction is $\sim$550 μb, while the experimental upper-limit cross section for the former reaction is about 21^{+38}_{-21} nb.
Conclusions: The intensity of suitable radioactive beams is not high enough at present to detect inverse fission. For the ^{124}Sn + ^{100}Mo reaction, the observed upper limits are below the estimates of current models for these reactions, probably due to fusion hindrance.

DOI: 10.1103/PhysRevC.85.044620 PACS number(s): 25.70.Jj, 25.85.−w, 25.60.Pj

I. INTRODUCTION

Nuclear fission is a notoriously difficult process to understand. In the more than 70 years since its discovery, we have made substantial progress in understanding several aspects of the fission process, but there are many questions to be answered. One long-standing hope has been to study "inverse fission" [1,2] in hopes of better understanding the macroscopic nuclear dynamics of the fission process, which involve large-scale collective motion. (Inverse fission is the fusing of two fission fragments to form a composite nucleus.) Comparisons of the relative dynamics of fusion and fission may help us understand the special features of each [3]. In addition, among the possible synthetic paths to new heavy nuclei is the process of inverse fission. (In a strict sense this is not really inverse fission, as the fusing fragments are not in their excited states during the reaction as they are when produced in fission, but the term is widely applied to this process.) A related process, "quasi inverse fission," is thought to offer possibilities for synthesizing n-rich heavy nuclei [4]. This paper addresses these physics motivations by providing a demonstration and a search for the feasibility of inverse fission.

Focusing on the inverse fission of uranium, some previous attempts have been made to simulate this process. The reaction of ^{48}Ca with ^{180}Hf produced the nucleus ^{225}U via the $3n$ evaporation channel [5] with a reported cross section of 130 nb. [The value of this cross section is anomalously low compared to similar reactions such as ^{48}Ca + ^{176}Yb and ^{48}Ca + ^{208}Pb, perhaps indicating that the single bombarding energy chosen was not optimal for producing the sought evaporation residue (EVR) ^{225}U]. In any case, this reaction is really too asymmetric to qualify as inverse fission. Attempts to fuse two ^{110}Pd nuclei to make ^{220}U failed to produce any ^{220}U evaporation residues with an upper-limit cross section of 10 nb [6,7]. (However EVRs were observed in this reaction at the Bass barrier despite the prediction [8] of the need for an extra push energy of 60 MeV). A variety of explanations [7,9–12] have been offered for this failure, not the least of which is the very neutron-deficient character of the completely fused system, ^{220}U, which makes it very fissionable. As pointed out by Lazarev and Oganessian [13], beams of neutron-rich fission fragments at energies of 4–5 MeV/nucleon, such as those formerly available at the Holifield Radioactive Ion Beam Facility (HRIBF), offer unique opportunities to study the inverse fission process.

To understand how we should carry out an inverse fission reaction, one needs to remember the general equations describing the synthesis of a heavy nucleus using complete fusion reactions. The cross section for producing an evaporation residue is

$$\sigma_{\mathrm{EVR}}(E_{\mathrm{c.m.}}) = \sum_{J=0}^{J_{\max}} \sigma_{CN}(E_{\mathrm{c.m.}}, J) W_{\mathrm{sur}}(E_{\mathrm{c.m.}}, J), \qquad (1)$$

where σ_{CN} is the complete fusion cross section and W_{sur} is the survival probability of the completely fused system. The complete fusion cross section can be written as

$$\sigma_{CN}(E_{\mathrm{c.m.}}) = \sum_{J=0}^{J_{\max}} \sigma_{\mathrm{capture}}(E_{\mathrm{c.m.}}, J) P_{CN}(E_{\mathrm{c.m.}}, J), \qquad (2)$$

where $\sigma_{\mathrm{capture}}(E_{\mathrm{c.m.}}, J)$ is the "capture" cross section at center-of-mass energy $E_{\mathrm{c.m.}}$ and spin J, and P_{CN} is the probability that the projectile-target system will evolve inside the fission saddle point to form a completely fused system rather than reseparating (quasifission).

The capture cross sections are adequately known [14]. Survival probabilities can be assessed by convenient methods [15].

TABLE I. Candidate reactions for the inverse fission of U.

Reaction	Product	σ_{fusion} (mb)	σ_{EVR} (mb)	HRIBF intensity (pps)	No. atoms (6 days)
^{48}Ca + ^{180}Hf	^{228}U	1.3	8×10^{-6}		
^{80}Ge + ^{150}Nd	^{230}U	1.7	1.2×10^{-3}	2×10^{4}	0.05
^{94}Rb + ^{137}Cs	^{231}U	0.4	7×10^{-4}	2×10^{4}	0.03
^{95}Sr + ^{136}Xe	^{231}U	1.9	2×10^{-3}	4×10^{4}	0.2
^{132}Sn + ^{100}Mo	^{232}U	7.4	2.7×10^{-2}	10^{5}	8.4
^{124}Sn + ^{100}Mo	^{224}U	21	4.8×10^{-5}	10^{10}	150
^{110}Pd + ^{110}Pd	^{220}U	2.3	1×10^{-5}		

The challenge in making estimates of inverse fission cross sections is to estimate P_{CN}, the fusion probability for nearly symmetric systems where fusion hindrance is expected to be large.

One approach is to simply rely on a self-consistent, successful model to make estimates of σ_{EVR} [15]. The application of this latter approach to several candidate inverse fission reactions is shown in Table I where we have assumed the optimum conditions for the (HI,2n) reactions. From the data in Table I, it would appear that the reactions of ^{124,132}Sn + ^{100}Mo might be suitable candidates for further studies of inverse fission at HRIBF.

II. EXPERIMENTAL METHOD

The measurements were carried out at the Holifield Radioactive Ion Beam Facility (HRIBF) at the Oak Ridge National Laboratory. Three irradiations of a ^{100}Mo target were made. The ^{100}Mo target (97% enriched) was 0.976 mg/cm^2 thick.

A. ^{132}Sn + ^{100}Mo

An irradiation of the ^{100}Mo target with 560 MeV ^{132}Sn was carried out. The apparatus is shown in Fig. 1. The beam passed through a 0.286 mg/cm^2 C degrader foil before striking the tilted (45°) ^{100}Mo target. All recoils formed were implanted in a single Al catcher foil of thickness 8.1 mg/cm^2 tilted an angle of 45° with respect to the beam direction. The duration of the irradiation was 7.2 days with a total dose of 3.0×10^{10} particles. Following irradiation, the Al catcher foil was shipped to Oregon State University for analysis.

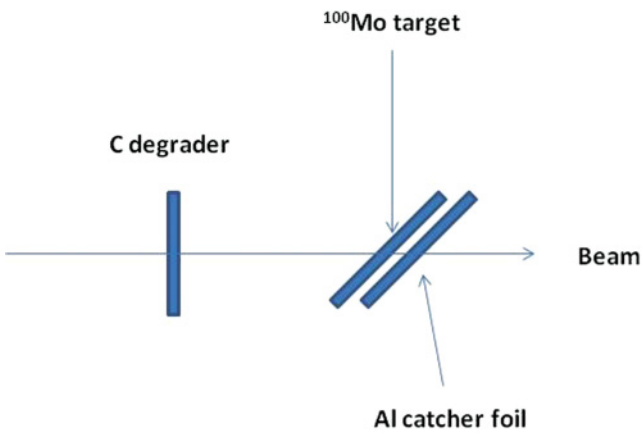

FIG. 1. (Color online) Schematic diagram of the irradiation setup for the ^{132}Sn + ^{100}Mo reaction.

At Oregon State University, the catcher foil was divided into two pieces. One piece was then counted in a 2π-geometry alpha spectrometer for 33 days to detect the presence of any implanted atoms. The background count rate in the spectrometer was 1.6×10^{-5} counts/s in the region from 6 to 8 MeV. No counts were observed above this background in the counting time of 2.9×10^{6} s. The other piece of the catcher foil was used to attempt a chemical separation of ^{230}U, which was not successful.

B. ^{124}Sn + ^{100}Mo

Two of the three irradiations involved the use of a ^{124}Sn beam. In the first irradiation, the ^{100}Mo target was mounted in the Oak Ridge evaporation residue detection system [16,17] (Fig. 2). Any evaporation residues (EVRs) produced passed through an ionization chamber mounted at zero degrees. Any potential EVRs were identified by time of flight and energy loss in the ion chamber. (See Refs. [16,17] for details of the operation of this detector.) The ionization-chamber and time-of-flight system was calibrated using ^{238}U beams of appropriate energies to mimic the EVRs passing through the apparatus. Two ^{124}Sn beam energies were used ($E_{\text{lab}} =$ 595 and 650 MeV) at beam intensities of 50 000–100 000 particles/s. (These energies correspond to 577 and 612 MeV "center-of-target" energies, i.e., $E_{\text{c.m.}} = 258$ and 273 MeV, respectively). The total beam doses were 4.4×10^{9} and 3.6×10^{9} particles. Upper-limit cross sections of 0.2 and 0.5 mb were measured for these two c.m. beam energies (258 and 273 MeV, respectively) [18].

Since this irradiation was carried out at low beam currents to allow use of the Oak Ridge evaporation residue detection system, we thought we should make a second irradiation at much higher beam currents to lower the upper-limit cross sections to a more physically meaningful level. The apparatus shown in Fig. 3 was installed in a general purpose beam line at HRIBF. The incident 531 MeV ^{124}Sn beam (center-of-target energy of 505 MeV) struck a 1.0 mg/cm^2 ^{100}Mo target tilted at 45° with respect to the beam direction. Any EVRs produced in the target recoiled out of the target and passed through a tilted 3.2 mg/cm^2 Al foil slowing down the EVRs. The EVRs

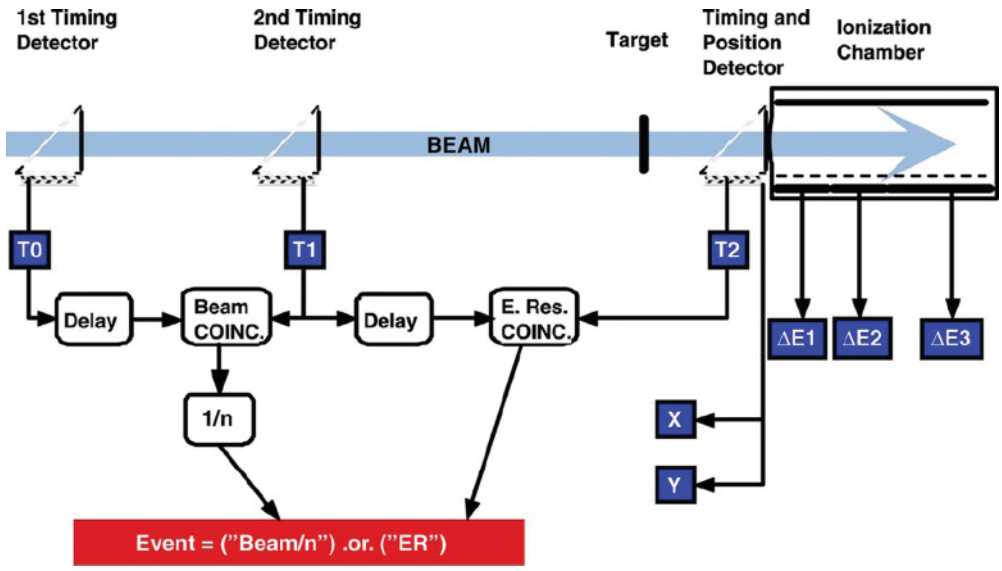

FIG. 2. (Color online) Schematic diagram of Oak Ridge evaporation residue detector system. From Ref. [16].

then stopped in a 0.81 mg/cm^2 Al foil, also tilted at 45° with respect to the beam direction. (TRIM simulations [19] suggest that 98.4% of the EVRs are caught in this second foil). This foil is viewed by two Si detectors mounted 2 cm from the beam path. The ^{124}Sn beam was pulsed (10 s on, 10 s off) and decay α particles from the stopped EVRs were detected during the beam-off periods. The geometrical efficiency of the detection system was 43%, as determined by Monte Carlo simulations. To pulse the beam on and off, a Faraday cup was installed in front of the apparatus shown in Fig. 3 and moved in and out of the beam. This device was used to sample the beam intensity and thus to integrate the beam dose. The total beam dose was 4.4×10^{14} particles. Following irradiation, the Al catcher foil was shipped to Oregon State University for analysis by alpha spectroscopy. This catcher foil was assayed by alpha spectroscopy for 24 days in a 2π-geometry alpha spectrometer.

III. DATA ANALYSIS

A. ^{132}Sn + ^{100}Mo

In the reaction of $E_{\rm lab} = 560$ MeV ^{132}Sn with ^{100}Mo, the center-of-target ^{132}Sn beam energy was $E_{\rm lab} = 510$ MeV ($E_{\rm c.m.} = 220$ MeV). This beam energy corresponds to the maximum of the predicted ^{100}Mo (^{132}Sn,2n)^{230}U reaction [15]. The expected decay sequence of ^{230}U is shown in Fig. 4. Secular equilibrium is quickly established between the ^{230}U and its progeny. This was demonstrated by producing a sample of ^{230}U using the ^{232}Th (p,3n)^{230}Pa reaction. The ^{230}Pa decays to ^{230}U. A typical spectrum of a ^{230}U sample ($\Delta t = 182000$ s) measured in our α spectroscopy setup is shown in Fig. 5. Thus we tried to detect any alpha particles emitted from the evaporation residues stopped in the catcher foil with $6000 \leqslant E_{\rm alpha} \leqslant 8000$ keV. The background count rate in the spectrometer in this energy region was 1.6×10^{-5} counts/s. The α spectrum of the catcher foil is shown in Fig. 6. The

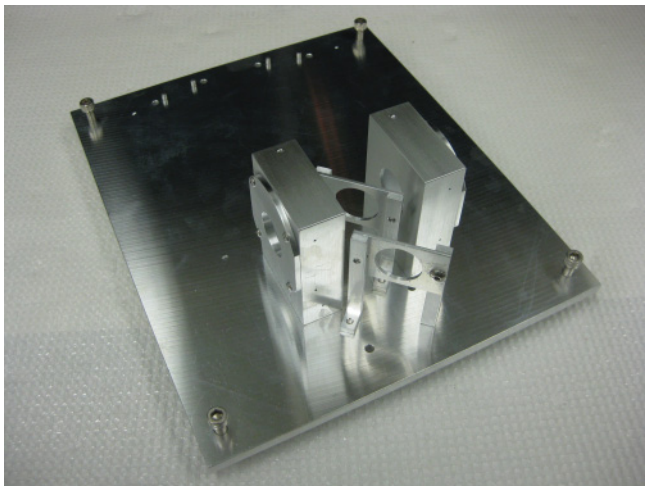

FIG. 3. (Color online) Photograph of apparatus used to measure yields for the ^{124}Sn + ^{100}Mo reaction.

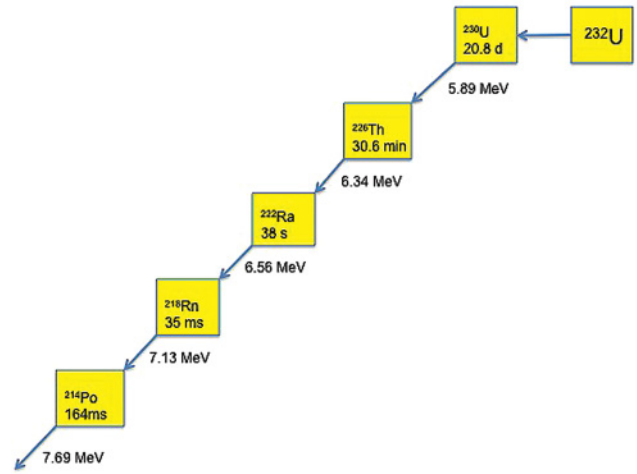

FIG. 4. (Color online) Expected decay scheme for ^{230}U.

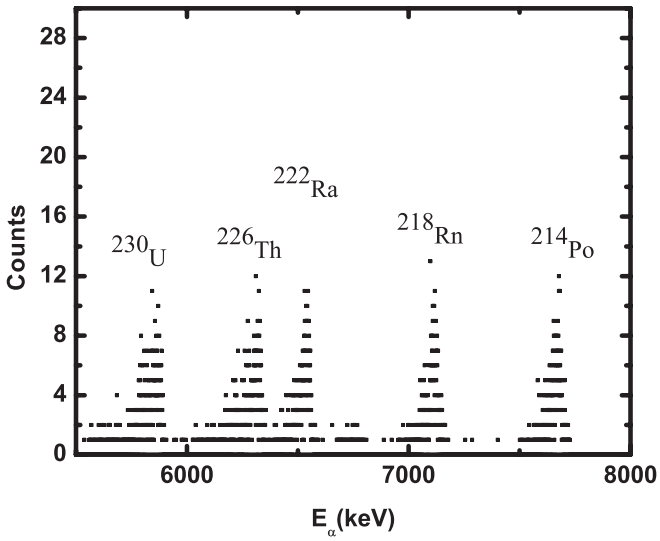

FIG. 5. Spectrum of a ^{230}U sample as counted in our apparatus.

counts in the spectrum at 6120 keV are due to a background peak from ^{252}Cf, which had been counted in the spectrometer previously. To estimate an upper limit for the presence of ^{230}U and its daughters in the measured spectra, we used the idea of the maximum detectable activity, L_D [20,21]. (L_D is the "true" net signal level which may *a priori* be expected to lead to detection [20].) Formally, for a system with a well known background,

$$L_D(\text{counts}) = 2.71 + 3.29\sqrt{\mu_b}, \tag{3}$$

where μ_b is the true mean background. L_D can be related to the upper-limit cross section as

$$L_D = K\sigma_{\text{upper}}, \tag{4}$$

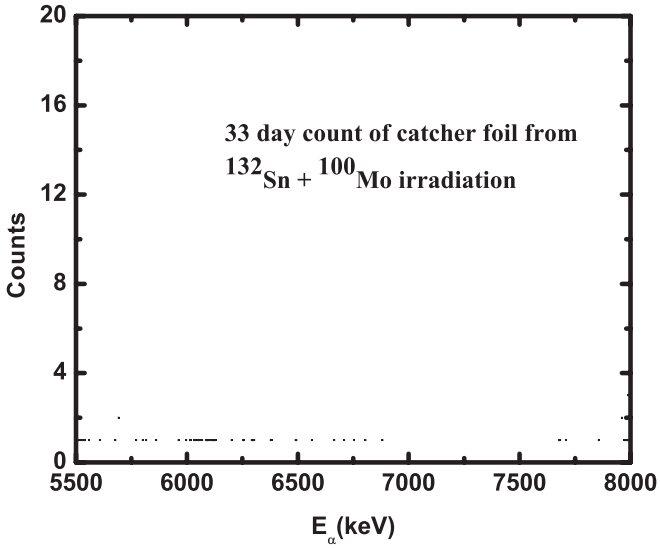

FIG. 6. Alpha spectrum (sample plus background) from counting the catcher foil in the ^{132}Sn + ^{100}Mo reaction.

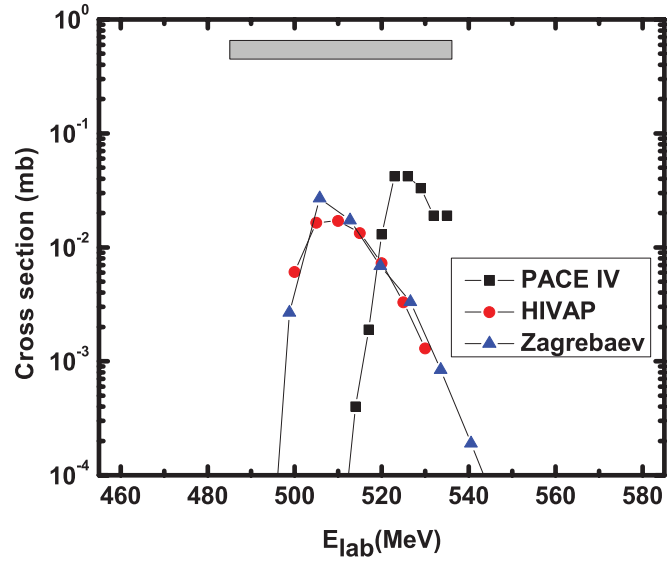

FIG. 7. (Color online) Predicted excitation functions for the ^{100}Mo(^{132}Sn,2n)^{230}U reaction. The shaded area roughly indicates the range of projectile energies covered in the target and the measured upper-limit cross section.

where K is given by

$$K = n\phi(1 - e^{-\lambda t_{\text{irr}}})\epsilon\frac{e^{-\lambda t_d}}{\lambda}(1 - e^{-\lambda\Delta t_c}). \tag{5}$$

In this equation, n is the number of target atoms/cm^2, ϕ is the average incident beam intensity in p/s, λ is the decay constant (s^{-1}) of the nuclide being produced, t_{irr} is the irradiation time, t_d is the decay time between the end of bombardment and the start of counting, and Δt_c is the counting time. ϵ is the detection efficiency. The upper-limit cross section for the ^{100}Mo(^{132}Sn,2n)^{230}U reaction is 550 μb.

To place this result in context, we show (in Fig. 7) the predicted cross sections for the production of ^{230}U in the irradiation of ^{100}Mo by ^{132}Sn. Three models were used to predict the expected (^{132}Sn,2n) reaction cross sections. They were (a) PACE IV, a web-based version of the statistical model code PACE [22,23]; (b) HIVAP [24,25], a frequently used model for predicting heavy element evaporation residue cross sections; and (c) the formalism (due to Zagrebaev [15]) used to construct Table I. The observed upper-limit cross section for the ^{100}Mo(^{132}Sn,2n)^{230}U reaction is 5.5×10^{-28} cm^2, i.e., 0.5 mb, which is greater than any of the predicted values of the cross section. Our search was not sensitive enough to detect the predicted cross sections.

Because we shall use these models to compare with other measurements, we need to describe these models in more detail. PACE [23] uses the Bass model [26] to calculate the complete fusion cross section and then treats the survival probabilities (in the competition between fission and particle emission) using Monte Carlo techniques to implement Hauser-Feshbach calculations. Angular momentum coupling is treated in the calculations. The transmission coefficients that describe the emission of neutrons, protons, and alpha particles were taken from optical model calculations. P_{CN} is assumed to be 1.

HIVAP is a statistical model code used extensively in describing the EVR cross sections in heavy-element synthesis reactions. It contains several more sophisticated physics options to calculate σ_{capture} and W_{sur}, but like PACE it is assumed that $P_{CN} = 1$. It is used primarily in describing hot fusion reactions, which are asymmetric. In the calculation of σ_{capture}, sub-barrier cross sections are calculated assuming an average interaction barrier and an assumed Gaussian distribution of interaction radii about some mean value. This "distribution of barriers" is adjusted to match experimental data. In addition, the deformation of the target nucleus is taken into account by an orientation averaging. In calculating the survival probabilities, shell effects on level densities (and their damping with excitation energy) are taken into account as well as angular momentum coupling. When applied to cold fusion reactions, HIVAP is known to overestimate the EVR cross sections significantly. Some researchers [27] have applied an arbitrary P_{CN} factor to normalize HIVAP calculations to experimental data.

The model used in Ref. [15] includes the use of coupled channels calculations to determine σ_{capture}, in which one takes into account inelastic excitations of the target and projectile nuclei along with a barrier distribution model. For example, for the ^{132}Sn + ^{100}Mo reaction, rotational excitations of ^{100}Mo ($\beta_2 = 0.244$, $\beta_4 = 0.023$, and $E_{2+} = 0.082$ MeV) and vibrational excitations of ^{132}Sn ($\lambda = 2$ and $\hbar\omega = 4.0$ MeV) were included. The nuclear potential was assumed to be a Woods-Saxon potential with $V_0^{\text{vol}} = -105$ MeV, $r_0^{\text{vol}} = 1.12$ fm, and $a^{\text{vol}} = 0.75$ fm. It was assumed that $P_{CN} = 1$ in all calculations. In calculating the survival probabilities, shell effects on level densities and their fade-out with excitation energy are treated using the formalism of Ref. [28]. The shell damping parameter γ was taken to be 0.061. One also treats the collective enhancement of level densities [29], and its deformation and excitation energy dependence [30].

B. ^{124}Sn + ^{100}Mo

As stated in Sec. II B above, the first studies of the ^{124}Sn + ^{100}Mo reaction were intended to detect "generic" evaporation residues, not necessarily complete fusion products. In Fig. 8, we show the predicted cross sections for the production of these generic evaporation residues as well as the product of the ^{100}Mo(^{132}Sn,2n)^{222}U reaction. The models used for this comparison are the same ones used in Fig. 7. The upper-limit cross sections for the production of generic evaporation residues were 0.2 and 0.5 mb, respectively, for the two studies with center-of-target energies $E_{\text{cot}} = 577$ and 612 MeV, respectively. These upper-limit cross sections are of the order of or below the predicted values of the cross sections.

We then undertook the study of the center-of-target energy $E_{\text{cot}} = 505$ MeV ($E_{\text{c.m.}} = 225$ MeV) ^{124}Sn + ^{100}Mo reaction. This beam energy should be at the predicted maximum of the ^{100}Mo(^{124}Sn,2n)^{222}U reaction (see Fig. 8). The decay scheme for ^{222}U is shown in Fig. 9. We focused our efforts on detecting the 2.46 s ^{214}Ra using in-beam alpha spectroscopy (during the 10 s beam-off period) and the 8.8 d ^{206}Po using post-irradiation alpha spectroscopy. From the in-beam spectroscopy

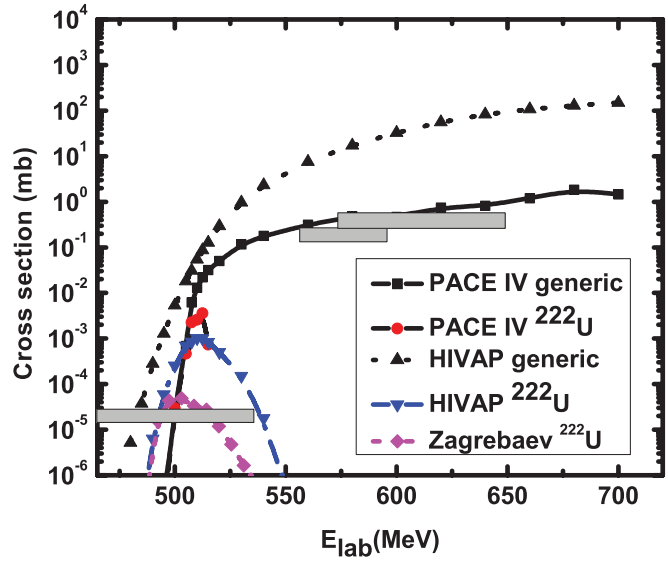

FIG. 8. (Color online) Predicted excitation functions for the ^{100}Mo(^{124}Sn,2n)^{230}U reaction. The shaded areas roughly indicate the range of projectile energies covered in the target and the measured upper-limit cross sections for the two experiments to measure the generic evaporation residue production and the one experiment to measure the yield of ^{222}U.

an upper limit for the cross section for the ^{100}Mo(^{124}Sn,2n) reaction of 21^{+38}_{-21} nb was found. (The uncertainties represent the traditional 68% confidence limits using Poisson statistics [31].) From the post-irradiation alpha-spectroscopic attempt to detect ^{206}Po, an upper limit for the cross section for the ^{100}Mo(^{124}Sn,2n) reaction of 270 nb was found.

IV. DISCUSSION

No evidence was found for the occurrence of inverse fission in any of the studies of the ^{124,132}Sn + ^{100}Mo reaction. For

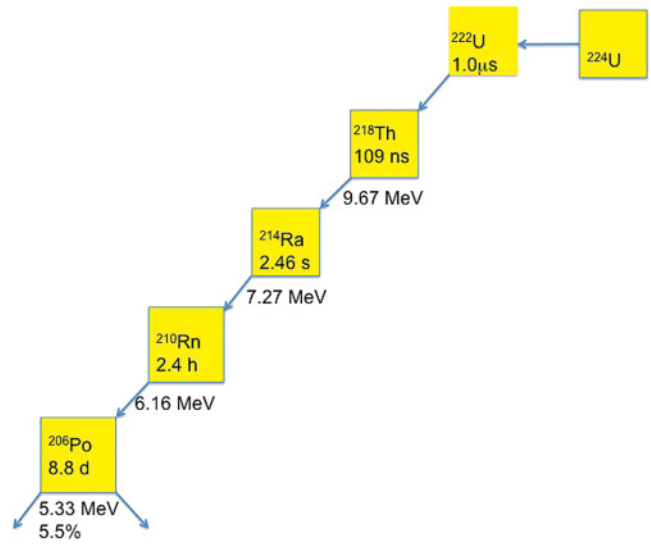

FIG. 9. (Color online) Expected decay scheme for ^{222}U.

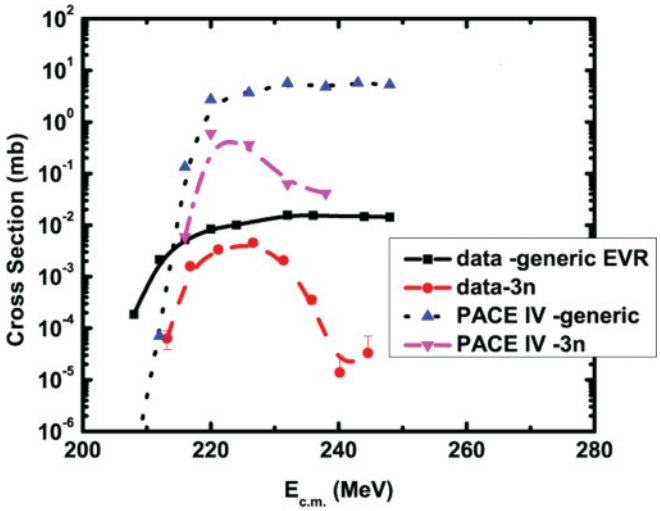

FIG. 10. (Color online) Comparison between measured and predicted (PACE IV) excitation functions for the ^{124}Sn + ^{96}Zr reaction.

the ^{100}Mo(^{132}Sn,2n)^{230}U reaction study, the experiment was not sensitive enough to detect the predicted reaction cross section. This was due to the fact that the actual average beam intensity was 5.4×10^4 particles per second (pps) (compared to the estimate of 10^5 pps in Table I) and the fact that the estimated production rates in Table I do not take into account the efficiency of detecting the produced residues. To improve upon this search would require increasing the production rate and detection efficiencies by a hundredfold. Since the HRIBF facility furnished the most intense ^{132}Sn beam available now and for the immediate future, a further attempt to detect inverse fission in this reaction will probably require extensive technical developments.

For the study of the ^{100}Mo(^{124}Sn,X) reaction to generate generic evaporation residues, the observed upper-limit cross sections are of the order of or below the predicted cross sections. Since this study was constrained by the acceptable

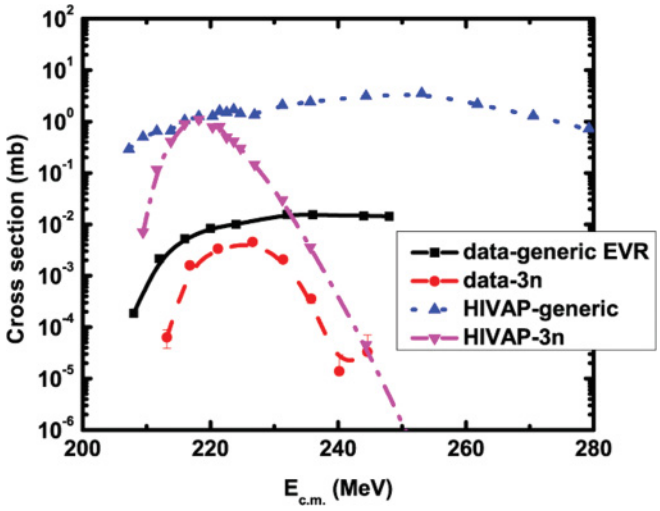

FIG. 11. (Color online) Comparison between measured and predicted (HIVAP) excitation functions for the ^{124}Sn + ^{96}Zr reaction.

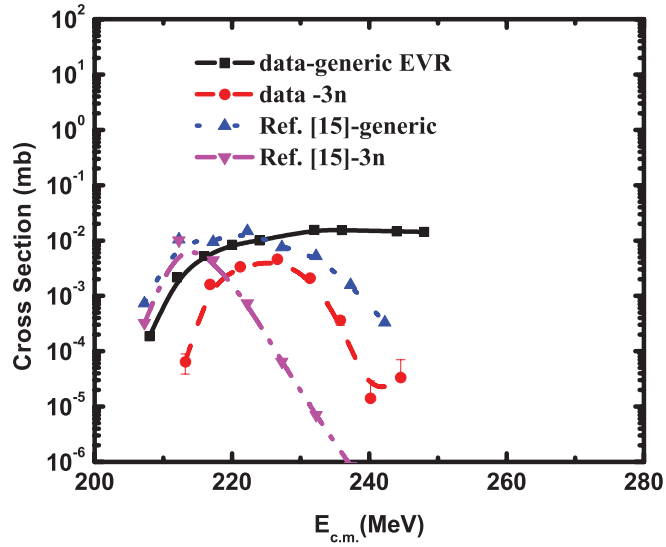

FIG. 12. (Color online) Comparison between measured and predicted [15] excitation functions for the ^{124}Sn + ^{96}Zr reaction.

counting rates of the Oak Ridge evaporation residue detection system [16,17], it would be feasible, with technical improvements, to further explore this system.

The most interesting case, however, is the study of the ^{100}Mo(^{124}Sn,2n)^{222}U reaction. The upper-limit cross sections, measured by in-beam spectroscopy and post-irradiation alpha spectroscopy, are lower than the predicted cross sections (Fig. 8). One problem in this comparison is that there is a substantial disagreement between the various predicted cross sections. The highest predicted cross sections come from PACE IV and HIVAP. These models do not include fusion hindrance (the P_{CN} factor). The model of Ref. [15], while not including fusion hindrance, predicts a substantially lower EVR cross section.

To gain insight into the issues involved,we turn to an analysis of the data from a similar, well-studied reaction: that of ^{124}Sn with ^{96}Zr [32,33]. There are measured values of the overall generic evaporation residue cross sections and data for specific reaction channels. These data are shown in Figs. 10–12 along with the predictions of the models used in Figs. 7 and 8. Once again, one notes that the models in both the PACE IV and HIVAP calculations significantly overestimate the magnitude of both the generic evaporation residue cross sections and the cross section for the (^{124}Sn,3n) reaction. The calculation model used in Ref. [15], with $P_{CN} = 1$, predicts values of the cross sections similar to or greater than those observed at lower excitation energies, but deviates from the measured data at higher energies.

TABLE II. Predicted values of P_{CN} for the ^{124}Sn + ^{96}Zr reaction.

Predicted values of P_{CN}	Reference
0.56	[4]
0.13	[36]
0.008	[27]
0.0002–0.004	[37]

In Table II, we collect various estimates of P_{CN} for the ^{124}Sn + ^{96}Zr reaction. In each case the model used in the calculations provided a good fit to the measured evaporation residue data.

What do we conclude from the comparison of various models with the measured evaporation residue cross sections for the ^{124}Sn + ^{96}Zr reaction and the deduced upper limits for the ^{124}Sn + ^{100}Mo reaction? Acceptable numerical models, i.e., those that have reasonable predictive power, correctly describing the EVR cross sections, may employ values of P_{CN} that differ by orders of magnitude. P_{CN} is not determined by indirect deductions using numerical models. P_{CN} should be measured directly [34,35]. The HIVAP code/model clearly overestimates the observed cross sections or upper limits for these near symmetric reactions, although it is generally known [25] to predict heavy-element formation cross sections (for asymmetric reactions) to within a factor of 2–3. The model of Ref. [15], which is probably the most sophisticated of the models studied, comes closest to correctly predicting the measured EVR cross sections, even though P_{CN} is taken to be 1. It may well be that very small deduced values of P_{CN} reflect other inadequacies in the models.

V. CONCLUSIONS

We conclude that: (a) We were not successful in our attempt to detect the inverse fission of uranium. (b) For the radioactive-beam-based attempt with the most n-rich nuclei, the ^{132}Sn + ^{100}Mo reaction, the beam intensities and detection sensitivities are orders of magnitude below those needed to observe the inverse fission process. (c) For the less n-rich system, the ^{124}Sn + ^{100}Mo reaction, the observed upper-limit cross sections are generally below the predictions of popular statistical models. (d) We suspect that the fusion hindrance in these nearsymmetric systems is underestimated, although an unambiguous determination of P_{CN} is not possible.

ACKNOWLEDGMENTS

This work was supported in part by the Office of High Energy and Nuclear Physics, Nuclear Physics Division, US Department of Energy, under Grant No. DE-FG06-97ER41026 and Contract No. DE-AC02-06CH11357.

[1] N. Bohr and J. A. Wheeler, Phys. Rev. **56**, 426 (1939).
[2] G. S. Janes, R. H. Levy, H. A. Bethe, and B. T. Feld, Phys. Rev. **145**, 925 (1966).
[3] J. R. Nix, Nucl. Phys. A **502**, 609c (1989).
[4] V. Zagrebaev and W. Greiner, Phys. Rev. C **78**, 034610 (2008).
[5] H. Gaggeler *et al*., Nucl. Phys. A **502**, 561c (1989).
[6] K. H. Schmidt and W. Morawek, Rep. Prog. Phys. **54**, 949 (1991).
[7] W. Morawek *et al*., GSI Report No. GSI-89-1 (unpublished), p. 38.
[8] J. P. Blocki, H. Feldmeier, and W. J. Swiatecki, Nucl. Phys. A **459**, 145 (1986).
[9] G. G. Adamian *et al*., Nucl. Phys. A **627**, 361 (1997).
[10] V. V. Volkov, Phys. At. Nucl. **62**, 1086 (1999).
[11] R. Moustabchir *et al*., Nucl. Phys. A **683**, 266 (2001).
[12] Y. Abe *et al*., Suppl. Prog. Theor. Phys. **146**, 104 (2002).
[13] Y. A. Lazarev and Y. T. Oganessian, in *Research with Fission Fragments* (World Scientific, Singapore, 1997).
[14] R. Yanez *et al*., Phys. Rev. C **82**, 054615 (2010).
[15] [http://nrv.jinr.ru/nrv/].
[16] D. Shapira, J. F. Liang, C. J. Gross, R. L. Varner, H. Amro, C. Harlin, J. J. Kolata, and S. Novotny, Nucl. Instrum. Methods Phys. Res., Sect. A **551**, 330 (2005).
[17] J. F. Liang *et al*., Phys. Rev. Lett. **91**, 152701 (2003).
[18] J. Beckerman, M.S. thesis, Oregon State University, 2010 (unpublished).
[19] J. F. Zeigler, J. P. Biersack, and M. D. Zeigler, *SRIM, The Stopping and Range of Ions in Matter* (Lulu Press, Morrisville, NC, 2011).
[20] L. A. Currie, Anal. Chem. **40**, 586 (1968).
[21] L. A. Currie, J. Radioanal. Nucl. Chem. **276**, 285 (2008).
[22] O. B. Tarasov and D. Bazin, Nucl. Instrum. Methods Phys. Res., Sect. B **204**, 174 (2003).
[23] A. Gavron, Phys. Rev. C **21**, 230 (1980).
[24] W. Reisdorf, Z. Phys. A **300**, 227 (1981).
[25] W. Reisdorf and M. Schaedel, Z. Phys. A **343**, 47 (1992).
[26] R. Bass, Nucl. Phys. A **231**, 45 (1974).
[27] R. N. Sagaidak, Eur. Phys. J. D **46**, 59 (2008).
[28] A. V. Ignatyuk, G. N. Smirenkin, and G. S. Tislin, Yad. Fiz. **21**, 485 (1975).
[29] V. I. Zagrebaev, Y. Aritomo, M. G. Itkis, Y. T. Oganessian, and M. Ohta, Phys. Rev. C **65**, 014607 (2001).
[30] A. R. Junghans *et al*., Nucl. Phys. A **629**, 635 (1998).
[31] K.-H. Schmidt, C.-C. Sahm, K. Pielenz, and H.-G. Clerc, Z. Phys. A **316**, 19 (1984).
[32] C. C. Sahm *et al*., Z. Phys. A **319**, 113 (1984).
[33] C. C. Sahm, H. G. Clerc, K. H. Schmidt, W. Reisdorf, P. Armbruster, F. P. Hessberger, J. G. Keller, G. Munzenberg, and D. Vermeulen, Nucl. Phys. A **441**, 316 (1985).
[34] B. B. Back, Phys. Rev. C **31**, 2104 (1985).
[35] R. S. Naik *et al*., Phys. Rev. C **76**, 054604 (2007).
[36] G. Fazio, G. Giardina, A. Lamberto, A. I. Muminov, A. K. Nasirov, F. Hanappe, and L. Stuttge, Eur. Phys. J. A **22**, 75 (2004).
[37] K. Siwek-Wilczynska, A. Borowiec, I. Skwira-Chalot, and J. Wilczynski, Int. J. Mod. Phys. E **17**, 12 (2008).